JCB Journal of Cell Biology

REPORT

Autophagosomal YKT6 is required for fusion with lysosomes independently of syntaxin 17

Takahide Matsui[1], Peidu Jiang[1], Saori Nakano[1], Yuriko Sakamaki[2], Hayashi Yamamoto[1], and Noboru Mizushima[1]

Macroautophagy is an evolutionarily conserved catabolic mechanism that delivers intracellular constituents to lysosomes using autophagosomes. To achieve degradation, lysosomes must fuse with closed autophagosomes. We previously reported that the soluble *N*-ethylmaleimide–sensitive factor attachment protein receptor (SNARE) protein syntaxin (STX) 17 translocates to autophagosomes to mediate fusion with lysosomes. In this study, we report an additional mechanism. We found that autophagosome–lysosome fusion is retained to some extent even in *STX17* knockout (KO) HeLa cells. By screening other human SNAREs, we identified YKT6 as a novel autophagosomal SNARE protein. Depletion of YKT6 inhibited autophagosome–lysosome fusion partially in wild-type and completely in *STX17* KO cells, suggesting that YKT6 and STX17 are independently required for fusion. YKT6 formed a SNARE complex with SNAP29 and lysosomal STX7, both of which are required for autophagosomal fusion. Recruitment of YKT6 to autophagosomes depends on its N-terminal longin domain but not on the C-terminal palmitoylation and farnesylation that are essential for its Golgi localization. These findings suggest that two independent SNARE complexes mediate autophagosome–lysosome fusion.

Introduction

Macroautophagy (referred to in this study as autophagy) is a highly conserved intracellular degradation system (Mizushima and Komatsu, 2011; Lamb et al., 2013; Abada and Elazar, 2014). Autophagy is achieved by well-organized membrane dynamics. Nucleation and elongation of the isolation membrane (also called the phagophore) lead to formation of the autophagosome, which then fuses with lysosomes. Whereas understanding of the molecular mechanisms of autophagosome formation has increased rapidly over the past decades, elucidation of those of autophagosome maturation, including the fusion step, began only recently. We and other groups identified syntaxin (STX) 17 as an autophagosomal SNARE protein (Qa-SNARE), which mediates autophagosome–lysosome fusion by interacting with SNAP29 (Qbc-SNARE) and VAMP7 or VAMP8 (R-SNARE; Itakura et al., 2012; Takáts et al., 2013). STX17 also binds to tethering factors such as homotypic fusion and protein sorting (HOPS), ATG14, and EPG5 to promote autophagosome–lysosome fusion (Jiang et al., 2014; Takáts et al., 2014; Diao et al., 2015; McEwan et al., 2015; Wang et al., 2016). Although the importance of STX17 in autophagosome–lysosome fusion has been confirmed in other studies (Guo et al., 2014; Cheng et al., 2015; Mauvezin et al., 2015, 2016; De Leo et al., 2016), recent research suggests that STX17 may not be essential for Parkin-mediated mitophagy, a process of selective degradation of mitochondria by autophagy (McLelland et al., 2016; Nguyen et al., 2016). Thus, it is possible that STX17 is not the sole autophagosomal SNARE protein.

To determine whether STX17 is an essential requirement, we generated *STX17* knockout (KO) HeLa cells and found that autophagosome–lysosome fusion was partially retained even in the absence of STX17. By screening human SNARE proteins, we identified YKT6 as a novel autophagosomal SNARE, which mediates autophagosome–lysosome fusion independently of STX17.

Results and discussion

Autophagosome–lysosome fusion is partially retained in *STX17* KO cells

To determine the requirement of STX17 in autophagosome–lysosome fusion precisely, we generated *STX17* KO HeLa cells using the CRISPR-Cas9 genome-editing method. In four independent *STX17* KO clones, the amount of microtubule-associated protein light chain 3 (LC3)-II increased even under growing

[1]Department of Biochemistry and Molecular Biology, Graduate School and Faculty of Medicine, The University of Tokyo, Tokyo, Japan; [2]Research Core, Tokyo Medical and Dental University, Tokyo, Japan.

Correspondence to Noboru Mizushima: nmizu@m.u-tokyo.ac.jp; T. Matsui's present address is Laboratory of Membrane Trafficking Mechanisms, Dept. of Developmental Biology and Neurosciences, Graduate School of Life Sciences, Tohoku University, Miyagi, Japan; P. Jiang's present address is Personalized Drug Therapy Key Laboratory of Sichuan Province, Sichuan Academy of Medical Sciences and Sichuan Provincial People's Hospital, School of Medicine, University of Electronic Science and Technology of China, Chengdu, China.

conditions, which was rescued by expression of Myc-STX17 (Fig. 1 A). These data are consistent with the previous notion that STX17 is required for autophagosome–lysosome fusion (Itakura et al., 2012; Takáts et al., 2013). However, treatment with the vacuolar ATPase inhibitor bafilomycin A_1 further increased the amount of LC3-II even in *STX17* KO cells, suggesting that autophagic flux partially remains in *STX17* KO cells. siRNA-mediated acute depletion of STX17 caused a more profound block in autophagic flux, as shown in our previous study (Itakura et al., 2012), suggesting that *STX17* KO cells might have adapted to the absence of STX17 (Fig. 1 B). We also measured the autophagic flux using the novel reporter GFP-LC3-RFP (Kaizuka et al., 2016). After synthesis, this reporter is cleaved by endogenous ATG4 proteases into equimolar amounts of GFP-LC3 and RFP. Although GFP-LC3 is degraded by autophagy, RFP remains in the cytosol. Accordingly, starvation treatment reduced the GFP/RFP ratio in WT cells but not in autophagy-deficient *ATG9A* KO cells (Fig. 1, C and D). However, a small reduction in the GFP/RFP ratio was observed in *STX17* KO cells, which was abolished by bafilomycin A_1 treatment. Collectively, these results suggest that autophagic flux is only partially blocked in *STX17* KO cells.

To directly analyze autophagosome–lysosome fusion, we examined colocalization between the autophagosomal marker LC3 and lysosomal marker LAMP-1. The number of LC3-positive punctate structures increased in *STX17* KO cells (Fig. 1, E and F). Some of these still colocalized with LAMP-1, although the rate of colocalization was decreased (Fig. 1, E and G), suggesting that autophagosomes can fuse with lysosomes in *STX17* KO cell. We also observed by electron microscopy that although undigested autophagosomes accumulated in *STX17* KO cells, bafilomycin A_1 treatment caused accumulation of partially digested autolysosomes not only in WT cells but also in *STX17* KO cells (Fig. 1, H and I). These data suggest that even in the absence of STX17, autophagosomes were able to fuse with lysosomes, although less efficiently, by a previously unknown mechanism.

YKT6 is a novel autophagosomal SNARE protein

To elucidate the STX17-independent mechanism of autophagosome–lysosome fusion, we screened 39 human SNARE proteins for their localization to unfused autophagosomes. For this purpose, we used TetON GFP-STX17ΔNTD cells, which express a dominant-negative form of STX17 (lacking the N-terminal domain) under the control of the tetracyclin promotor (Uematsu et al., 2017). Overexpressed GFP-STX17ΔNTD localizes to completed autophagosomes and blocks autophagosome–lysosome fusion, leading to accumulation of unfused autophagosomes. Among the 39 Myc-tagged SNAREs, STX17, SNAP29, and YKT6 extensively colocalized with GFP-STX17ΔNTD (Figs. 2 A and S1, A and B). As STX17 and SNAP29 localize on autophagosomes (Itakura et al., 2012; Takáts et al., 2013), we focused on YKT6 as a candidate for a novel autophagosomal SNARE.

YKT6 is an R-SNARE protein conserved from yeast to humans and is anchored to membranes via palmitoylation and farnesylation (see Fig. 5 A; Fukasawa et al., 2004). YKT6 is involved in multiple membrane fusion processes such as ER–Golgi traffic (with STX5, GS28, and BET1; McNew et al., 1997; Zhang and Hong, 2001; Fukasawa et al., 2004), intra-Golgi transport (Volchuk et al., 2004), early or recycling endosome to trans-Golgi network transport (Tai et al., 2004), Golgi to vacuole transport (Kweon et al., 2003), homotypic vacuole fusion (with Vam3, Vam7, and Vti1; Ungermann et al., 1999; Dilcher et al., 2001), and exosome fusion with the plasma membrane (Ruiz-Martinez et al., 2016). In addition, it has been suggested that YKT6 is involved in phagophore formation and Cvt vesicle–vacuole fusion in *Saccharomyces cerevisiae* (Dilcher et al., 2001; Nair et al., 2011). However, the precise localization and function of YKT6 during autophagosome–lysosome fusion have not been directly determined.

First, we investigated the localization of YKT6 during autophagy in mouse embryonic fibroblasts (MEFs). GFP-YKT6 showed cytosolic localization under growing conditions but formed punctate structures upon starvation in WT MEFs but not in autophagy-deficient *Fip200* KO MEFs (Figs. 2 B and S1, C and D). Most of these GFP-YKT6 puncta were colocalized with LC3. As GFP-YKT6 showed a high background cytosolic signal that might mask some punctate signals, we also used prepermeabilized cells in which the cytosol was washed out before fixation. In these cells, GFP-YKT6 puncta colocalized with LC3 and partially with LAMP-1 but not with the isolation membrane markers FIP200 and WIPI2 (Fig. 2, B and C). GFP-YKT6 puncta also colocalized with LC3 and almost completely overlapped with the mRuby3-tagged transmembrane domain of STX17, which translocates to autophagosomes upon starvation (Fig. 2, D and E; Itakura et al., 2012; Tsuboyama et al., 2016). The YKT6 and LAMP-1 double-positive structures were mostly LC3 positive (Fig. S1, E and F). These results suggest that GFP-YKT6 localizes on autophagosomes and autolysosomes but not on isolation membranes and LC3-negative lysosomes.

In contrast with *Fip200* KO MEFs, GFP-YKT6 puncta were formed in *Atg3* KO and *Atg5* KO MEFs under starvation conditions (Fig. S1, C and D). This result was not unexpected because these cells contain autophagosome-like structures to which STX17 can also localize (Tsuboyama et al., 2016), and this result supports the notion that YKT6 localizes to autophagosomes.

Finally, we determined whether endogenous YKT6 also localizes on autophagosomes using a membrane flotation method (Fig. 2 F). In a stepwise OptiPrep gradient, autophagosomes containing STX17, LC3-II, and p62 were collected in fraction 3 only after autophagy induction by Torin 1, an mTORC1 inhibitor. Endogenous YKT6 was also detected in fraction 3 after Torin 1 treatment. Other organelle markers such as LAMP-1, ERGIC53 (ERGIC), SEC61β (ER), and TOMM20 (mitochondria) were not detected in this fraction. The signals of LC3-II, p62, and YKT6 in fraction 3 were enhanced in *STX17* KO cells (Fig. 2 F), in which unfused autophagosomes accumulated (Fig. 1, H and I). In contrast, the endogenous YKT6 signal in fraction 3 of Torin 1–treated cells was reduced by simultaneous treatment with wortmannin, an inhibitor of PtdIns 3-kinase, which is required for isolation membrane formation (Fig. S1 G; Blommaart et al., 1997). These results suggest that endogenous YKT6 is present on autophagosomes.

Autophagosome–lysosome fusion is completely blocked in cells lacking both YKT6 and STX17

YKT6 is involved in multiple membrane-fusion pathways. As expected, 5-d knockdown of YKT6 impaired degradation of the

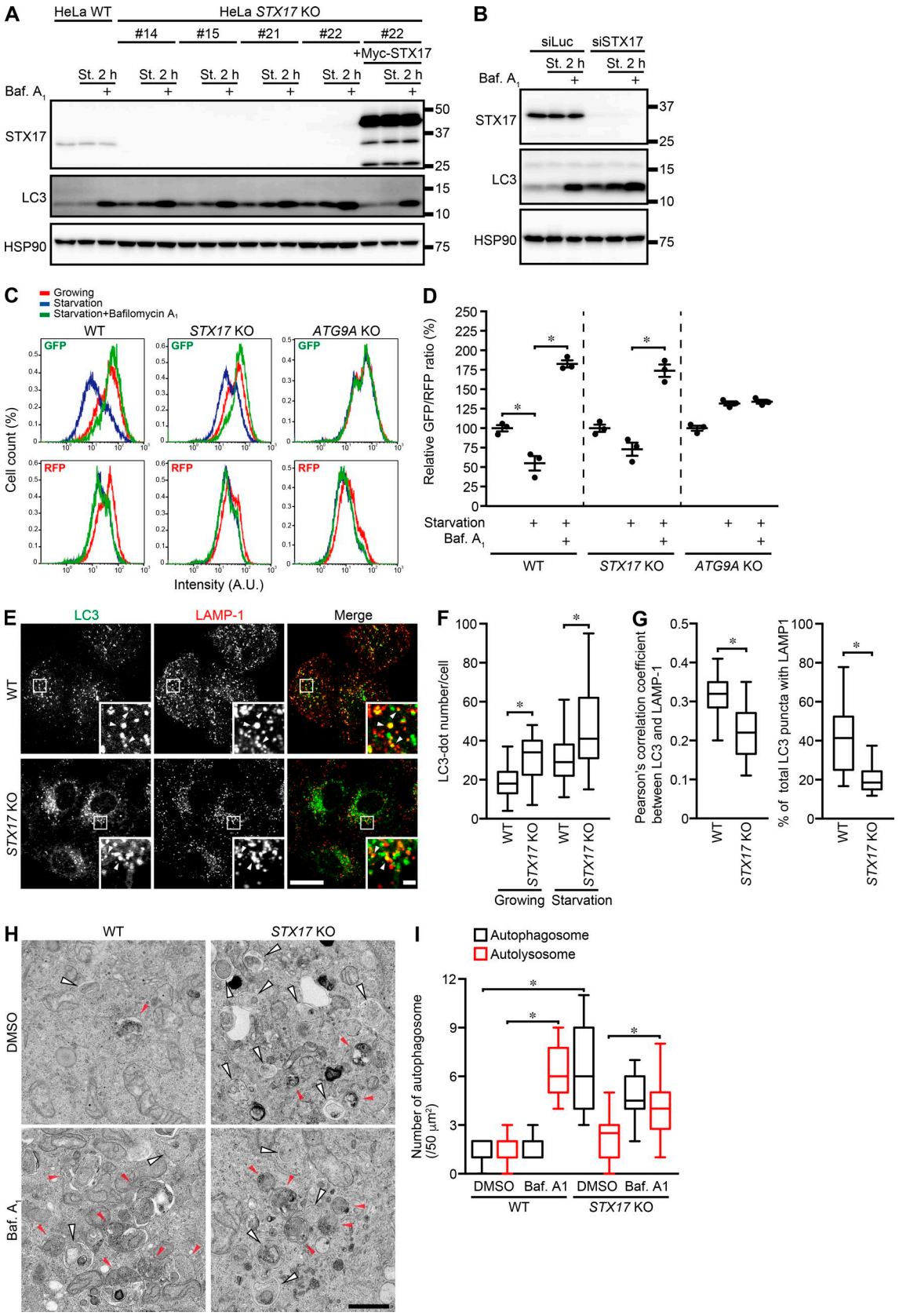

Figure 1. ***STX17* KO cells show only a partial defect in autophagosome–lysosome fusion. (A)** WT and *STX17* KO HeLa cells (four independent clones and one rescued clone) were cultured in growing or starvation medium (St.) for 2 h with or without 100 nM bafilomycin A_1 (Baf A_1). **(B)** WT HeLa cells were transfected with siLuciferase (siLuc; as a negative control) or siSTX17. After 3 d, cells were transfected with the same siRNAs again and cultured for another 2 d. Molecular masses are given in kilodaltons. **(C and D)** WT, *STX17* KO, and *ATG9A* KO HeLa cells stably expressing GFP-LC3-RFP were cultured in growing or

EGF receptor, cathepsin D maturation, and the glycosylation of LAMP-1, suggesting that long-term knockdown of YKT6 leads to dysfunction of endolysosomes (Fig. S2, A and B). In contrast, 3-d knockdown of YKT6 did not show any apparent defects in these indicators of lysosomal function. However, even with intact lysosomal function, 3-d knockdown of YKT6 caused a partial block in autophagic flux in WT cells, suggesting that YKT6 is partially required for autophagy independently of lysosomal function (Figs. 3 A and S2 C). The differential effect of 3-d knockdown of YKT6 on lysosomal function and autophagosome–lysosome fusion is not unexpected because lysosomal enzymes that had already been delivered to lysosomes could function even after depletion of YKT6. In addition, 3-d knockdown of YKT6 almost completely blocked the remaining autophagic flux in *STX17* KO cells. Overexpression of STX17 and YKT6 did not restore the block in autophagic flux in YKT6-depeleted and *STX17* KO cells, respectively (Fig. S2, D and E). Thus, YKT6 regulates autophagic flux independently of STX17. Furthermore, knockdown of YKT6 significantly increased the number of LC3-positive puncta and decreased the colocalization rate between LC3 and LAMP-1 in WT cells (Fig. 3, B–D, WT), and there was an additive effect with *STX17* KO (Fig. 3, B–D). We previously showed that in *ATG3* KO cells, autophagosome-like structures can be generated (Tsuboyama et al., 2016). Fusion of these structures with lysosomes were also blocked by depletion of YKT6 and STX17 (Fig. S2, F and G). Electron microscopy analysis also showed that knockdown of YKT6 increased the number of undigested autophagosomes in both WT and *STX17* KO cells, and depletion of both YKT6 and STX17 reduced the number of autolysosomes (Fig. 3, E and F). To further show that STX17 and YKT6 are required for fusion, we performed an in vitro fusion assay (Barysch et al., 2010). GFP-LC3–positive autophagosomes prepared from siRNA-treated HeLa cells were mixed with LysoTracker red–stained lysosomes prepared from *ATG9A* KO HeLa cells (Fig. 3 G). Depletion of either YKT6 or STX17 from autophagosomes partially inhibited colocalization between GFP-LC3 and LysoTracker red signals, and depletion of both YKT6 and STX17 showed an additive effect (Fig. 3, H and I). Together, these results suggest that YKT6 mediates fusion between autophagosomes and lysosomes independently of STX17 and that both are required for the fusion process.

YKT6 forms a SNARE complex with SNAP29 and STX7

As YKT6 is an R-SNARE, it should interact with Qa-, Qb-, and Qc-SNAREs to mediate membrane fusion (Hong, 2005; Jahn and Scheller, 2006). Among Qb- and Qc-SNAREs, YKT6 could interact with BET1 (Qc) and SNAP29 (Qbc; Fig. S3 A). It is known that the YKT6–BET1 interaction is involved in ER–Golgi transport (Zhang and Hong, 2001), whereas the YKT6–SNAP29 interaction has not been previously reported. Autophagic flux was reduced by 5-d but not 3-d knockdown of BET1 (Fig. S3 B). However, 5-d BET1 knockdown also affected EGF receptor degradation, cathepsin D maturation, and LAMP-1 glycosylation, suggesting that the defect in autophagy in BET1 knockdown cells is caused by lysosomal dysfunction (Fig. S3, C and D). However, 3-d knockdown of SNAP29 partially blocked autophagic flux without affecting lysosomal function (Fig. S2, B, C, and H), confirming that SNAP29 functions in the autophagy pathway independently of the endocytic pathway (Itakura et al., 2012).

We next sought to identify a Qa-SNARE functioning together with YKT6 and SNAP29, but we found that YKT6 and SNAP29 could interact with almost all Qa-SNAREs (Fig. S3, E and F). Given that YKT6 is located on autophagosomes, we searched for Qa-SNAREs that localized to lysosomes and identified STX7 as a candidate (Fig. S3 G). STX7 has previously been reported as a lysosomal SNARE that regulates late endosome–lysosome fusion (Mullock et al., 2000; Pryor et al., 2004). However, 3-d knockdown of STX7 did not affect lysosomal function but decreased autophagic flux slightly in WT cells and profoundly in *STX17* KO cells (Figs. 4 A and S2, B, C, and I). Furthermore, depletion of STX7 also increased the number of LC3-positive puncta and decreased colocalization between LC3 and LAMP-1 in both WT and *STX17* KO cells (Fig. 4, B–D) as well as in *ATG3* KO cells (Fig. S2, F and G). The partial defect in autophagic flux in YKT6 knockdown cells was not enhanced by simultaneous knockdown of STX7, whereas knockdown of YKT6 and STX17 showed an additive effect, suggesting that YKT6 and STX7 function in the same pathway, which is distinct from the STX17 pathway (Fig. 4 E). As previously reported (Kim et al., 2001), STX7 but not YKT6 interacted with HOPS components such as VPS11 and VPS39 (Fig. S3 H). Thus, YKT6 likely mediates autophagosome–lysosome fusion together with the Qbc-SNARE SNAP29 and the Qa-SNARE STX7 independently of STX17.

Next, we determined whether YKT6 forms a complex with SNAP29 and STX7. Our immunoprecipitation assay demonstrated that only a small amount of endogenous YKT6 was precipitated with FLAG-STX7, but when Myc-SNAP29 was overexpressed, a larger amount of YKT6 was precipitated together with Myc-SNAP29 but not STX17, suggesting that YKT6 could form a ternary complex with SNAP29 and STX7 (Fig. 4 F). Furthermore, STX7 interacted with SNAP29 and YKT6 in *STX17* KO cells (Fig. 4 G), and STX17 interacted with SNAP29 and VAMP8 in YKT6 knockdown cells (Fig. 4 H). These results further suggest that these two complexes act independently.

starvation medium for 4 h with or without 100 nM bafilomycin A_1. Cells were analyzed by flow cytometry. Representative histograms (C) and quantification of the GFP/RFP intensity ratio (D) are shown. Data represent means ± SEM of three independent experiments. **(E–G)** Cells were cultured in starvation medium for 2 h, and colocalization between endogenous LC3 and LAMP-1 (indicated by white arrowheads) was determined (E). Colocalization was determined in >15 cells by calculating Pearson's correlation coefficient and actual colocalization rate (G). The number of LC3 punctate structures per cell (in >30 cells) was quantified (F). The solid bars indicate median, the boxes indicate the interquartile range (25th to 75th percentile), and the whiskers indicate the upper and lower quartiles. The statistical analyses were performed by two-sided Student's unpaired *t* test. Bars: (main images) 20 µm; (insets) 2 µm. **(H and I)** Cells were starved for 2 h with or without 100 nM bafilomycin A_1 and analyzed by conventional electron microscopy. Autophagosomes and autolysosomes are indicated by white and red arrowheads, respectively. The number of autophagosomes and autolysosomes in >10 cells was quantified (I). *, $P < 0.01$. **(C, D, H, and I)** One-way ANOVA and Tukey's test were used. Bar, 1 µm.

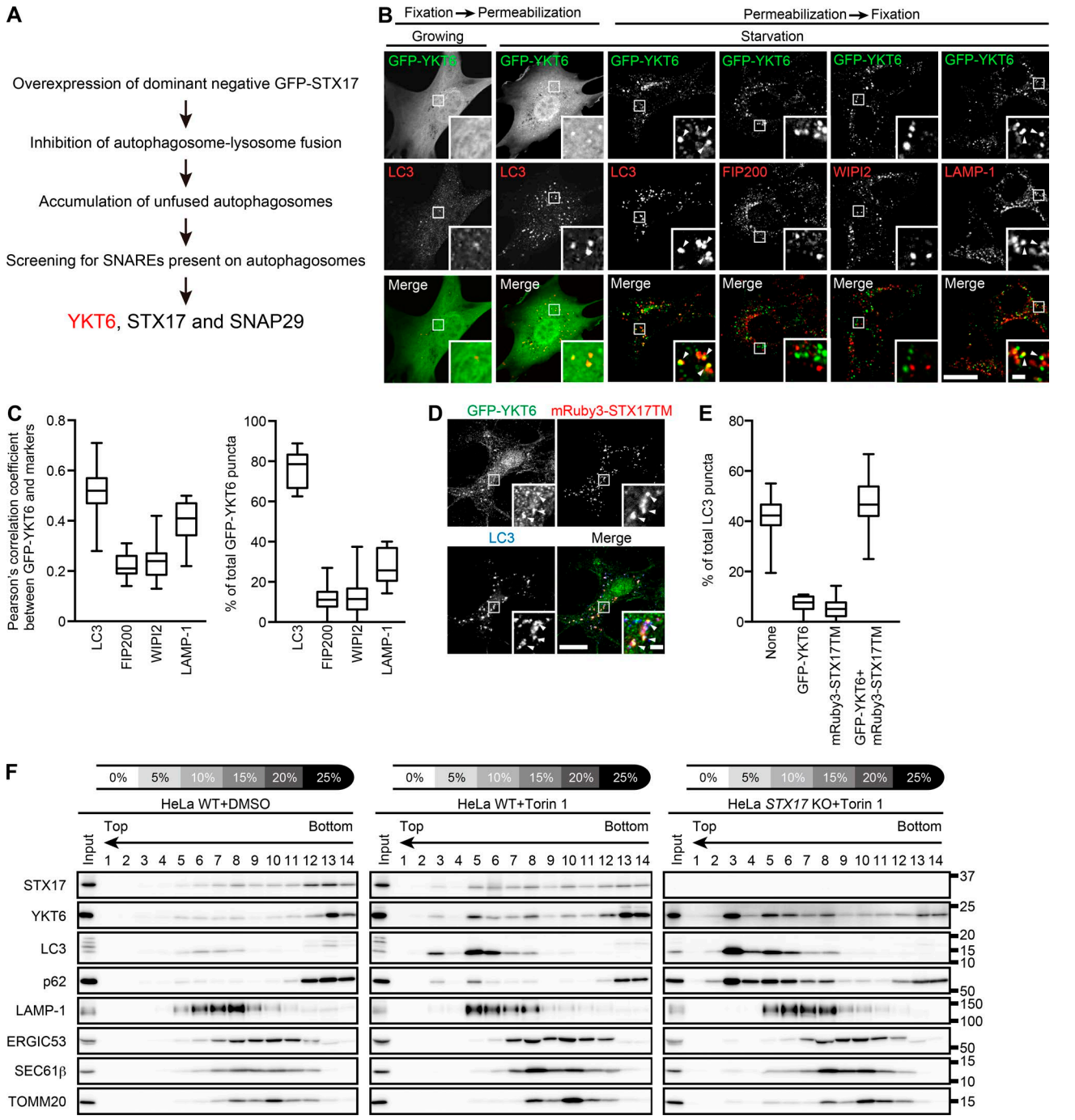

Figure 2. **YKT6 is a novel autophagosomal SNARE protein. (A)** Strategy to identify autophagosomal SNARE proteins. **(B and C)** MEFs stably expressing GFP-YKT6 were cultured in growing or starvation medium for 1 h and fixed. Where indicated, cells were prepermeabilized before fixation. Colocalization between GFP-YKT6 and the indicated markers (indicated by arrowheads) was quantified in >15 cells as in Fig. 1 G. **(D and E)** MEFs stably expressing GFP-YKT6 and mRuby3-STX17TM were starved for 1 h and immunostained with anti-GFP and anti-LC3 antibodies. Colocalization between GFP-YKT6, mRuby3-STX17TM, and LC3 is denoted by arrowheads. The YKT6- or STX17-positive ratio of total LC3 structures was quantified in >15 cells (E). Bars: (main images) 20 µm; (insets) 2 µm. **(F)** WT and *STX17* KO HeLa cells were treated with or without 250 nM Torin 1 for 2 h, and cell homogenates were subjected to OptiPrep flotation analysis. Molecular masses are given in kilodaltons.

YKT6 localization on autophagosomes is dependent on its N-terminal region

YKT6 is anchored to membranes via palmitoylation and farnesylation of the two cysteine residues (Cys194 and Cys195) in the most C-terminal five-amino-acid residues CCAIM immediately downstream of the SNARE domain (Fig. 5 A; Fukasawa et al., 2004). However, GFP-YKT6C194S/C195S mutant, which is unable to localize on Golgi (Fukasawa et al., 2004), could still translocate to autophagosomes (Fig. 5, B and C). In contrast, the Golgi-resident mutant GFP-YKT6F42E (Tochio et al., 2001; Fukasawa et al., 2004) showed a perinuclear Golgi pattern with no colocalization with LC3 (Fig. 5, B and C). Thus, the recruitment

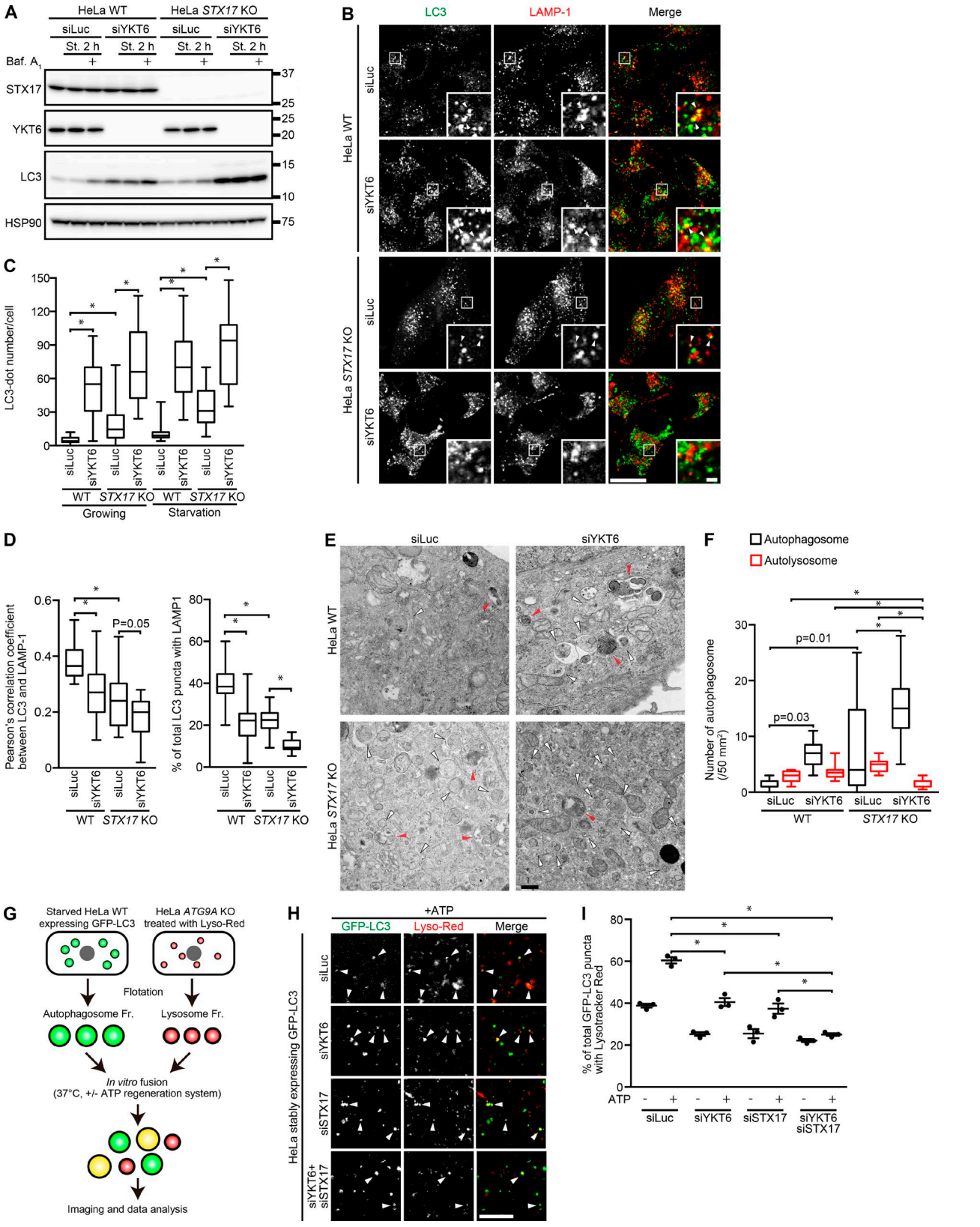

Figure 3. **Depletion of YKT6 and STX17 completely inhibits autophagosome–lysosome fusion. (A)** WT and *STX17* KO HeLa cells were transfected with siLuciferase (siLuc) or siYKT6. After 3 d, cells were cultured in growing or starvation medium (St.) for 2 h with or without 100 nM bafilomycin A_1 (Baf. A_1). Molecular masses are given in kilodaltons. **(B–D)** Cells were prepared as in A, starved for 2 h, and immunostained with anti-LC3 and anti–LAMP-1 antibodies. Colocalization between LC3 and LAMP-1 (indicated by arrowheads) was quantified in >15 cells as in Fig. 1 G (D). The number of LC3 punctate structures per cell (in >30 cells) was quantified (C). Bars: (main images) 20 µm; (insets) 2 µm. **(E and F)** Cells were prepared as in A, starved for 2 h, and analyzed by conventional electron microscopy. Autophagosomes and autolysosomes are indicated by white and red arrowheads, respectively. The number of autophagosomes and

mechanism of YKT6 to Golgi and autophagosomes is different. We further found that GFP-YKT6-SNARE (containing the SNARE domain and C-terminal CCAIM sequence) showed a perinuclear pattern with little colocalization with LC3, whereas GFP-YKT6-Longin clearly colocalized with LC3 puncta (Fig. 5, B and C). These results suggest that the N-terminal longin domain is required and sufficient for the autophagosomal targeting of YKT6. However, as Myc-YKT6-Longin as well as Myc-YKT6C194S/C195S could not restore autophagic flux in YKT6-depleted cells, C-terminal palmitoylation and farnesylation is required for mediating autophagosome–lysosome fusion (Fig. 5 D).

YKT6 can interact with several Qa-SNAREs including STX17 (Fig. S3 E), and the interaction between YKT6 and STX17 was also enhanced by overexpression of FLAG-SNAP29 (Fig. S3 I). Thus, YKT6 could form a ternary complex with SNAP29 and STX17, which likely occurs on the same autophagosomes (Fig. 2, D and E). However, recruitment of YKT6 and of STX17 to autophagosomes is not interdependent; GFP-YKT6 colocalized with LC3 in *STX17* KO cells (Fig. 5 E), and Myc-STX17 colocalized with LC3 in YKT6 knockdown cells (Fig. 5 F). The former result was consistent with the previous OptiPrep gradient data showing that endogenous YKT6 was detected in autophagosome-containing fraction 3 in *STX17* KO cells (Fig. 2 F). Thus, YKT6 and STX17 can be independently recruited to autophagosomes.

Conclusion

Based on the findings of this study, we propose that two distinct SNARE complexes mediate autophagosome–lysosome fusion. One complex is the previously reported STX17–SNAP29–VAMP7/8 (Itakura et al., 2012; Takáts et al., 2013); the other, discovered in this study, is YKT6–SNAP29–STX7 (Fig. 5 G). These two complexes have Qa- and R-SNARE proteins on the opposite membranes. Why this fusion event requires two distinct SNARE sets is unknown, but may be (A) simply to make this event efficient, or (B) to fuse autophagosomes with distinct populations of lysosomes or endosomes if the localization of VAMP7/8 and STX7 is different. The latter may be apparent in large cells such as neurons, in which mature lysosomes are enriched in the cell body (Overly and Hollenbeck, 1996; Lee et al., 2011). Additionally, the role of STX17–SNAP29–YKT6 (Fig. S3 I) is currently unknown. It may be involved in homotypic fusion of autophagosomes (or autolysosomes), although this is not observed frequently. Alternatively, because some STX17 and YKT6 could also be present on lysosomes, STX17 and YKT6 on lysosomes may, respectively, interact with YKT6 and STX17 on autophagosomes to form a third trans-SNARE complex mediating autophagosome–lysosome fusion. Additional future experiments will be required to address this point.

Autophagosomal SNAREs should be recruited to autophagosomes immediately before or after the closure of autophagosomes to prevent premature lysosomal fusion that may leak lysosomal enzymes to the cytoplasm. The mechanism of this temporal regulation remains to be elucidated even for STX17. In the case of YKT6, the N-terminal region, which mainly contains the longin domain, is required for its recruitment to autophagosomes. The longin domain is found in YKT6, SEC22B, and VAMP7 among the SNARE family (Rossi et al., 2004). The longin domain has been considered to be a negative regulatory module because it inhibits the formation of a SNARE complex by intramolecular binding to the SNARE domain (Tochio et al., 2001). However, the longin domain of VAMP7 is important for proper post-Golgi sorting to endocytic vesicles by binding to the ArfGAP Hrb (Pryor et al., 2008), and the longin domain of YKT6 (but not that of SEC22B) is required for localization to a specialized compartment in neurons (Hasegawa et al., 2003). Thus, there may be an unknown autophagosomal factor that interacts with the longin domain of YKT6. It also remains a possibility that there is a common mechanism that is shared by YKT6 and STX17 to be recruited to autophagosomes.

Materials and methods

Cell culture

HeLa cells, HEK293 cells, and MEFs were cultured in DMEM (D6546; Sigma-Aldrich) supplemented with 10% FBS (172021; Sigma-Aldrich), 2 mM L-glutamine (25030-081; Gibco), and 50 µg/ml penicillin and streptomycin (15070-063; Gibco) in a 5% CO_2 incubator. For starvation treatment, cells were washed twice with PBS and incubated in amino acid–free DMEM (048-33575; Wako Pure Chemical Industries) without serum. *Fip200* KO (Gan et al., 2006), *Atg3* KO (Sou et al., 2008), and *Atg5* KO (Kuma et al., 2004) MEFs and *ATG9A* KO, *ATG3* KO (Tsuboyama et al., 2016), and TetON GFP-STX17ΔNTD HeLa (Uematsu et al., 2017) cells have been described previously. For bafilomycin A_1, Torin 1, or wortmannin treatment, cells were cultured with 100 nM bafilomycin A_1 (B1793; Sigma-Aldrich), 250 nM Torin 1 (4247; Tocris Bioscience), or 200 nM wortmannin (W1628; Sigma-Aldrich) for 2 h, respectively. To visualize lysosomes, cells were cultured with 50 nM LysoTracker red DND-99 (L-7528; Thermo Fisher Scientific) for 1 h.

Plasmids

cDNAs encoding human STX7, STX17, STX17TM, STX18, SNAP29, Vti1B, and VAMP8 and mouse VAMP7 were obtained as previously described (Itakura et al., 2012). Other human SNARE cDNAs were amplified by PCR from total cDNA of HEK293 or SH-SY5Y cells. YKT6 fragments and their point mutants were generated by a standard PCR method or an inverse PCR, respectively. The cDNAs were inserted into pMRXIP (provided by S. Yamaoka, Tokyo Medical and Dental University, Tokyo, Japan; Saitoh et al.,

autolysosomes was quantified in >10 cells (F). Bar, 500 nm. **(G–I)** A schematic model of the in vitro autophagosome–lysosome fusion assay (G). An autophagosome-containing fraction (Fr.) from siRNA-treated HeLa cells expressing GFP-LC3 and a lysosome-containing fraction from LysoTracker red (Lyso-Red)–treated *ATG9A* KO HeLa cells were mixed with or without the ATP-regeneration system. Representative confocal pictures (with ATP) are shown (H). Colocalization between GFP-LC3 and LysoTracker red (indicated by arrowheads) was quantified (I). Data represent means ± SEM of three independent experiments. Bar, 10 µm. *, $P < 0.01$ (one-way ANOVA and Tukey's test).

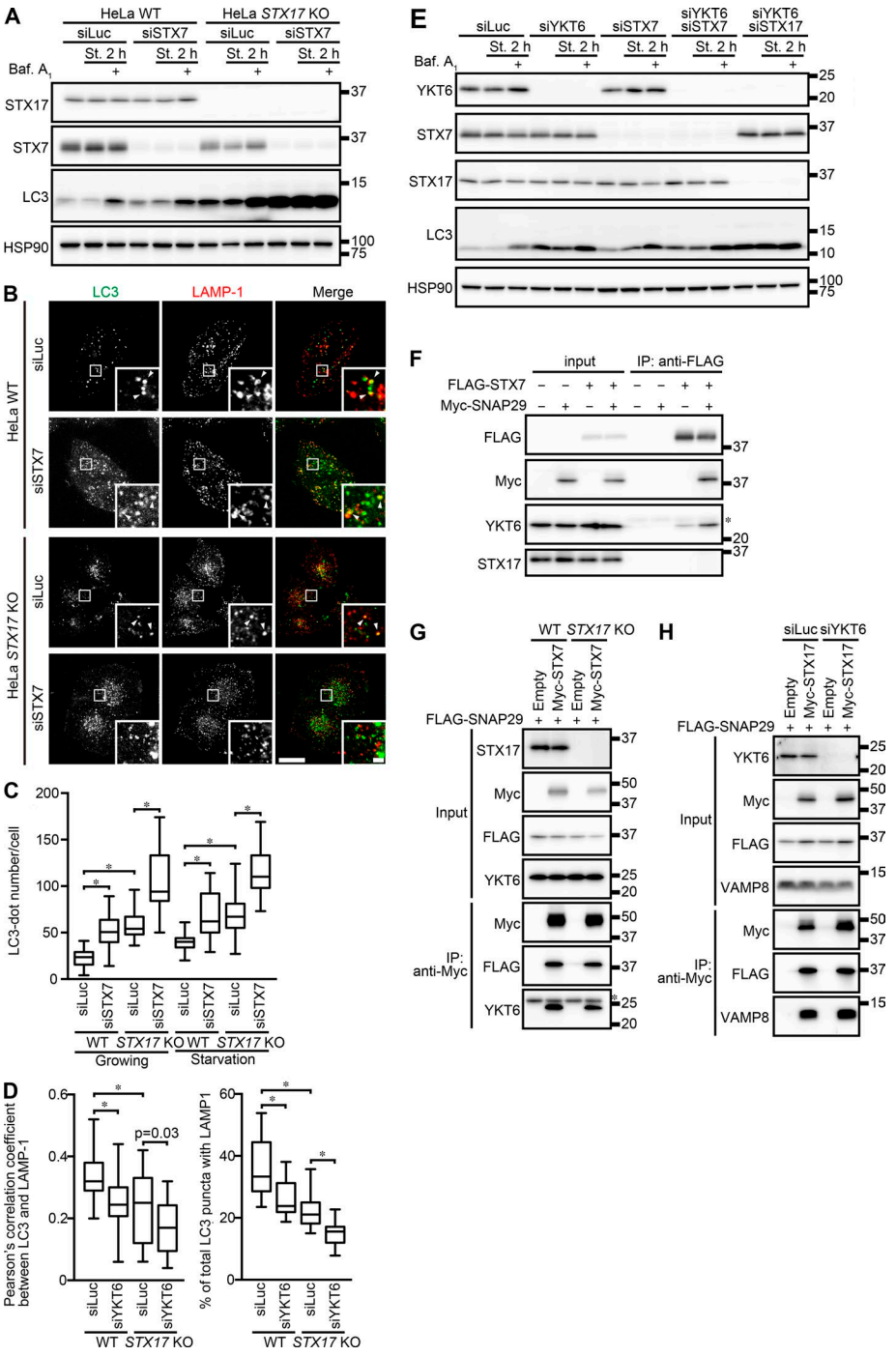

Figure 4. **YKT6 forms a complex with SNAP29 and STX7. (A)** WT and *STX17* KO HeLa cells were transfected with siLuciferase (siLuc) or siSTX7. After 3 d, cells were cultured in growing or starvation medium (St.) for 2 h with or without 100 nM bafilomycin A_1 (Baf. A_1). **(B–D)** Cells were prepared as in A without bafilomycin A_1 and immunostained with anti-LC3 and anti–LAMP-1 antibodies. Colocalization between LC3 and LAMP-1 (indicated by arrowheads) was quantified in >15 cells as in Fig. 1 G (D). Quantification of the number of LC3 punctate structures per cell (determined in >20 cells) is shown in C. *, $P < 0.01$ (one-way ANOVA and Tukey's test). Bars: (main images) 20 µm; (insets) 2 µm. **(E)** HeLa cells were transfected with indicated siRNAs. After 3 d, cells were cultured in growing or starvation medium for 2 h with or without 100 nM bafilomycin A_1. **(F)** HEK293T cells transiently expressing the indicated constructs were starved for 1 h. Cell lysates were immunoprecipitated (IP) with anti-FLAG antibody. **(G)** WT and *STX17* KO HeLa cells transiently expressing the indicated constructs were starved for 1 h. Cell lysates were immunoprecipitated with anti-Myc antibody. Asterisks indicate positions of IgG light chains. **(H)** WT HeLa cells were transfected with siLuciferase or siYKT6. After 2 d, cells were transfected with the indicated constructs and cultured for another 1 d. Cell lysates were analyzed as in G. Molecular masses are given in kilodaltons.

2002) together with enhanced GFP, 3×Myc, or codon-optimized mRuby3 (modified from pKanCMV-mClover3-mRuby3; 74252; Addgene). pSpCas9 (BB)-2A-GFP (pX458; 48138; Addgene) was used for establishment of a KO cell line.

Antibodies and reagents

For immunoblotting, mouse monoclonal anti-YKT6 (sc-365732; Santa Cruz Biotechnology, Inc.), anti-FLAG M2 (F1804; Sigma-Aldrich), anti–β-actin (A2228; Sigma-Aldrich), anti-HSP90 (610419; BD), anti-BET1 (sc-136390; Santa Cruz Biotechnology, Inc.), rabbit polyclonal anti-LC3 (which recognizes both LC3A and LC3B; Kabeya et al., 2000), anti-STX17 (HPA001204; Sigma-Aldrich), anti-p62 (PM045; MBL), anti-ERGIC53 (E1031; Sigma-Aldrich), anti-SEC61β (15087-1-AP; ProteinTech), anti-TOMM20 (sc-11415; Santa Cruz Biotechnology, Inc.), anti-FLAG (F7425; Sigma-Aldrich), anti-Myc (2272; Cell Signaling Technology), anti-SNAP29 (111-302; Synaptic Systems), anti-STX7 (A304-512A; Bethyl Laboratories), goat polyclonal anti–cathepsin D (sc-6486; Santa Cruz Biotechnology, Inc.), and sheep polyclonal anti-EGF receptor (20-ES04; Fitzgerald Industries International) were used as primary antibodies. Anti–mouse (111-035-003) and anti–rabbit (111-035-144) HRP-conjugated IgG (Jackson ImmunoResearch Laboratories, Inc.) were used as secondary antibodies. For immunostaining, mouse monoclonal anti-LC3 (which

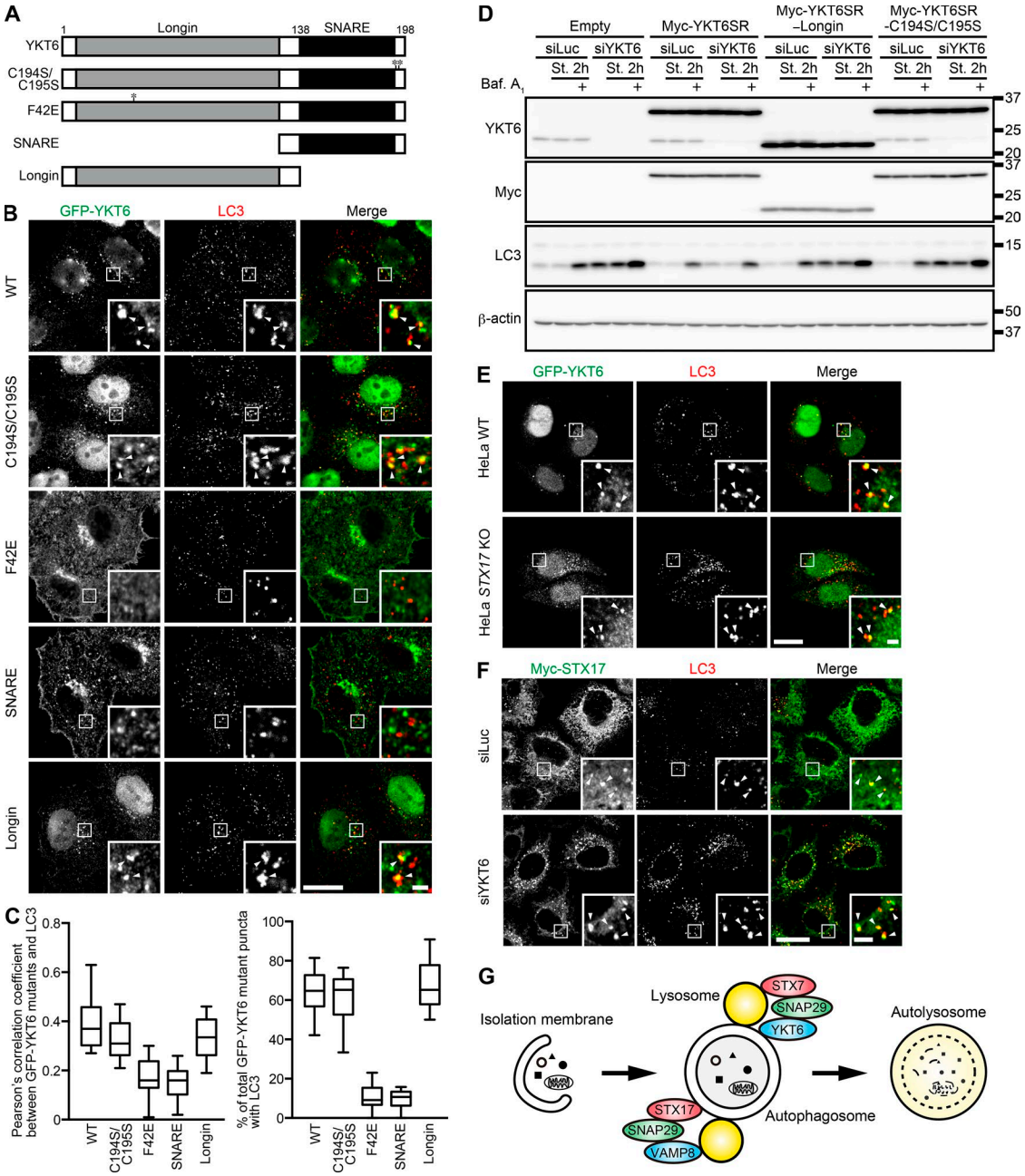

Figure 5. **YKT6 localization on autophagosomes is dependent on its N-terminal region. (A)** The domain-based structure of YKT6 and its mutant used in this study. Asterisks indicate positions of mutated residues. **(B and C)** HeLa cells stably expressing indicated constructs were cultured in starvation medium (St.) for 2 h and prepermeabilized before fixation. Cells were immunostained with anti-GFP and anti-LC3 antibodies. Colocalization between GFP-YKT6 mutants and LC3 (indicated by arrowheads) was quantified in >15 cells as in Fig. 1 G (C). **(D)** WT HeLa cells stably expressing the indicated siRNA-resistant Myc-YKT6 (Myc-YKT6SR) mutants were transfected with siLuciferase (siLuc) or siYKT6. After 3 d, cells were cultured in growing or starvation medium for 2 h with or without 100 nM bafilomycin A_1 (Baf. A_1). Molecular masses are given in kilodaltons. **(E)** WT and *STX17* KO HeLa cells stably expressing GFP-YKT6 were prepared as in B, and colocalization between GFP-YKT6 and LC3 was determined (indicated by arrowheads). **(F)** HeLa cells stably expressing Myc-STX17 were transfected with siLuciferase or siYKT6. After 3 d, cells were cultured in starvation medium for 2 h and immunostained with anti-Myc and anti-LC3 antibodies. Colocalization between Myc-STX17 and LC3 is denoted by the arrowheads. Bars: (main images) 20 µm; (insets) 2 µm. **(G)** A model of SNARE proteins in autophagosome–lysosome fusion. YKT6 and STX17 localize to autophagosomes independently of each other. YKT6 and STX17 form a SNARE complex with SNAP29–STX7 and SNAP29–VAMP8, respectively, and mediate autophagosome–lysosome fusion.

recognizes mainly LC3A; CTB-LC3-2-IC; Cosmo Bio), rabbit polyclonal anti-FIP200/RB1CC1 (17250-1-AP; ProteinTech), anti-WIPI2 (SAB4200400; Sigma-Aldrich), and anti-Myc (16286-AP; ProteinTech) were used as primary antibodies. Alexa Fluor 488–conjugated anti–mouse IgG (A-11001) and anti–rabbit IgG (A-11008), Alexa Fluor 568–conjugated anti–mouse IgG (A-11004) and anti–rabbit IgG (A-11011), and Alexa Fluor 660–conjugated anti–rabbit IgG (A-21074; Molecular Probes) were used as secondary antibodies. Rabbit polyclonal anti–LAMP-1 (ab24170; Abcam) and anti-GFP (A6455; Thermo Fisher Scientific) were used for immunoblotting

and immunofluorescence. For transient transfection, Lipofectamine 2000 transfection reagent (11668019; Thermo Fisher Scientific) and ViaFect transfection reagent (E4981; Promega) were used, according to the manufacturer's instructions.

RNAi

Stealth RNAi oligonucleotides were purchased from Thermo Fisher Scientific. The sequences used were as follows: human YKT6 siRNA antisense, 5′-GGTGTGGTCATTGCTGACAATGAAT-3′, and sense, 5′-ATTCATTGTCAGCAATGACCACACC-3′; and human BET1 siRNA antisense, 5′-AGTTGTGGAATCAAATTG TGAATCC-3′, and sense, 5′-GGATTCACAATTTGATTCCACAACT-3′. The siRNA oligonucleotides for human STX17 (HSS123732 antisense, 5′-AATTAAGTCCGCTTCTAAGGTTTCC-3′, and sense, 5′-GGAAACCTTAGAAGCGGACTTAATT-3′), SNAP29 (HSS113853 antisense, 5′-GGCTGACAACCAAAGTGGACAAGTT-3′, and sense, 5′-AACTTGTCCACTTTGGTTGTCAGCC-3′), and STX7 (HSS112239 antisense, 5′-TGATGAGACTGATAATCGCAACTCC-3′, and sense, 5′-GGAGTTGCGATTATCAGTCTCATCA-3′) were reported previously (Itakura et al., 2012). The stealth RNAi oligonucleotides were transfected into cells using Lipofectamine RNAiMAX (13778150; Thermo Fisher Scientific) according to the manufacturer's instructions. 3 d after transfection, cells were harvested (short-term knockdown) or were again transfected with the same siRNA and cultured for an additional 2 d before analysis (long-term knockdown).

Retroviral infections and generation of stable cell lines

HEK293T cells were transiently transfected using Lipofectamine 2000 with retrovirus vectors, pCG-gag-pol, and pCG-VSV-G (provided by T. Yasui, The National Institute of Biomedical Innovation, Health and Nutrition, Osaka, Japan). After 48 h, culture medium containing retrovirus was collected and filtered through a 0.45-µm syringe filter unit (SLHV033RB; EMD Millipore). Cells were cultured with retrovirus and 8 µg/ml polybrene (H9268; Sigma-Aldrich). Uninfected cells were removed by 1 µg/ml puromycin (P8833; Sigma-Aldrich).

Establishment of *STX17* KO HeLa cell lines

CRISPR guide RNA (gRNA) sequences designed to target the human *STX17* gene were cloned into the pX458 vector. The target sequences were human *STX17* 1, 5′-TAATTAGACACCATTTAA CGTGG-3′ (upstream of exon 5), and human *STX17* 2, 5′-GAT GCTTAACATTGAGAGTGTGG-3′ (downstream of exon 6). These gRNA sequences were designed to delete exons 5 and 6. HeLa cells were transfected using ViaFect with the pX458 vector carrying the above gRNA sequences. After 24 h, GFP-positive cells were isolated using a cell sorter (MoFlo Astrios EQ; Beckman Coulter), and single clones were obtained. Clones with mutations in both alleles were identified by genomic DNA sequencing and immunoblotting. The genomic PCR primers in HeLa cells were as follows: human *STX17* forward, 5′-CACCTAGGCTGGAGTGCAGC-3′, and human *STX17* reverse, 5′-CTGAGGCGGGTGGATCATGA-3′.

Immunoprecipitation and immunoblotting

Cell lysates were prepared in a lysis buffer (50 mM Tris-HCl, pH 7.5, 150 mM NaCl, 1 mM EDTA, 1% Triton X-100, 1 mM Na_3VO_4, and protease inhibitor cocktail [complete EDTA-free protease inhibitor; 05056489001; Roche]). After centrifugation at 17,700 *g* for 10 min, the supernatants were subjected to immunoprecipitation using anti-Myc 9E10 (MMS-150R; Covance) or anti-GFP (D153-3; MBL) in combination with protein G Sepharose (17061801; GE Healthcare) or anti-FLAG M2 affinity gel (A2220; Sigma-Aldrich). Precipitated immunocomplexes were washed three times in washing buffer (50 mM Tris-HCl, pH 7.5, 150 mM NaCl, 1 mM EDTA, and 1% Triton X-100) and boiled in sample buffer. Samples were subsequently separated by SDS-PAGE and transferred to Immobilon-P polyvinylidene difluoride membranes (IPVH00010; EMD Millipore). Immunoblot analysis was performed with the indicated antibodies and visualized with Immobilon Western chemiluminescent HRP substrate (WBKLS0500; EMD Millipore).

Immunocytochemistry

Cells grown on coverslips were washed with PBS and fixed in 4% paraformaldehyde in PBS for 10 min at room temperature. Fixed cells were permeabilized with 50 µg/ml digitonin (D141; Sigma-Aldrich) in PBS for 5 min, blocked with 3% BSA in PBS for 30 min, and then incubated with primary antibodies for 1 h. After washing three times with PBS, cells were incubated with Alexa Fluor 488/568/660–conjugated goat anti–mouse or anti–rabbit IgG secondary antibodies for 1 h. The coverslips were observed using a confocal laser microscope (FV1000 IX81; Olympus) with a 100× oil-immersion objective lens (1.40 NA; Olympus) and captured with FluoView software (Olympus). For prepermeabilization, cells were treated with 50 µg/ml digitonin in KHM buffer (125 mM potassium acetate, 25 mM Hepes, pH 7.2, and 2.5 mM magnesium acetate) for 1 min for MEFs or 3 min for HeLa cells at room temperature before fixing. After washing twice with KHM buffer, cells were fixed. The number of punctate structures and colocalization rate were determined using FIJI software (ImageJ; National Institutes of Health; Schindelin et al., 2012). Small structures (<800 nm) were removed using an open operation. The images were processed using Photoshop CS6 (Adobe).

Cell fractionation

Cells from four 10-cm dishes were harvested and washed twice with ice-cold PBS. The cell pellets were collected after centrifugation at 700 *g* for 5 min and resuspended in 2 ml ice-cold homogenization buffer (250 mM sucrose, 20 mM Hepes-KOH, pH 7.4, 1 mM EDTA, and complete EDTA-free protease inhibitor). Cells were then disrupted by N_2 cavitation (800 psi; Parr Instrument). The homogenized cells were centrifuged twice at 3,000 *g* for 10 min to remove cell debris and undisrupted cells. The supernatant was diluted with an equal volume of 50% OptiPrep (1114542; Sigma-Aldrich) in homogenization buffer. Discontinuous OptiPrep gradients were generated in SW41 tubes (344059; Beckman Coulter) by overlaying the following OptiPrep solutions in homogenization buffer: 2.4 ml of the diluted supernatant in 25% OptiPrep, 1.8 ml in 20%, 2 ml in 15%, 2 ml in 10%, 2.0 ml in 5%, and 2.0 ml in 0%. The gradients were centrifuged at 150,200 *g* in SW41 Ti rotors (Beckman Coulter) for 3 h, and then 14 fractions (0.8 ml each) were collected from the top. Proteins in each fraction were isolated by TCA precipitation. The final pellet was suspended in sample buffer and heated at 95°C for 5 min.

In vitro autophagosome–lysosome fusion assay

The assay was performed as described previously with some modifications (Barysch et al., 2010). In brief, autophagosome-containing fractions (fraction 3) from starved WT HeLa stably expressing GFP-LC3 as well as lysosome-containing fractions (fraction 8) from 50 nM LysoTracker red–treated *ATG9A* KO HeLa were collected as described above. Both fractions were mixed with the same volume of homogenization buffer (250 mM sucrose and 20 mM Hepes-KOH, pH 7.4) followed by centrifugation at 50,000 *g* for 15 min to precipitate membrane. The precipitated membrane was suspended with 1 µg/ml cytosol from WT HeLa cells in homogenization buffer and mixed in the presence or absence of ATP regeneration system. The samples were incubated at 37°C by gently shaking. After 1 h, the membranes were collected by centrifugation at 50,000 *g* for 15 min and suspended with homogenization buffer. The samples were placed on coverslips and observed using a confocal laser microscope. Acquired images were analyzed by FIJI software. More than 3,000 puncta were analyzed in each sample.

EGF receptor degradation assay

HeLa cells were cultured at 90% confluence in serum-starved DMEM for 22 h and then were incubated with 100 ng/ml EGF (059-07873; Wako Pure Chemical Industries) containing DMEM for varying time periods. Cell lysates were analyzed by immunoblotting with the indicated antibodies.

Flow cytometry

Cells stably expressing GFP-LC3-RFP were cultured in the indicated medium for 4 h. The dishes were placed on ice immediately after trypsinization, and the cells were transferred to siliconized 1.5-ml tubes (131-615CH; Watson Bio Lab) with ice-cold PBS. The cells were centrifuged at 2,300 *g* for 3 min, resuspended in ice-cold PBS containing 7-AAD (51-68981E; BD), and analyzed using a flow cytometer (EC800; Sony) equipped with 488-nm and 561-nm lasers. At least 30,000 events for each sample were acquired. Data were processed using Kaluza software (Beckman Coulter). 7-AAD–positive dead cells were removed.

Electron microscopy

Cells were cultured on cell-tight C-2 cell disks (MS-0113K; Sumitomo Bakelite) and fixed in 2.5% glutaraldehyde (G015; TAAB Laboratories Equipment) in 0.1 M phosphate buffer, pH 7.4, for 2 h on ice. The cells were washed with 0.1 M phosphate buffer, pH 7.4, three times, postfixed in 1% osmium tetroxide in 0.1 M phosphate buffer, pH 7.4, for 2 h, dehydrated, and embedded in epon 812 according to a standard procedure. Ultrathin sections were stained with uranyl acetate and lead citrate and observed using an H-7100 (Hitachi) or JEM-1010 (JEOL) electron microscope.

Statistical analysis

Two groups of data were evaluated by unpaired two-tailed Student's *t* test, and multiple comparisons were performed by one-way ANOVA followed by the Tukey's test. Data distribution was assumed to be normal, but this was not formally tested.

Online supplemental material

Fig. S1 shows additional YKT6 localization data. Fig. S2 shows the effect of short- or long-term knockdown of YKT6, SNAP29, or STX7 on autophagic flux and lysosomal function. Fig. S3 shows the results of a screen for SNARE proteins interacting with YKT6.

Acknowledgments

We thank Shoji Yamaoka for the retroviral vectors and Teruhito Yasui for the pCG-VSV-G and pCG-gag-pol plasmids. We thank all members of the laboratory, especially Ikuko Koyama-Honda, for discussion.

This work was supported by Japan Society for the Promotion of Science Grant-in-Aid for Scientific Research on Innovative Areas (grant 25111005) and Japan Science and Technology Agency Exploratory Research for Advanced Technology (ERATO; grant JPMJER1702) to N. Mizushima.

The authors declare no competing financial interests.

Author contributions: T. Matsui, H. Yamamoto, and N. Mizushima designed the project. T. Matsui performed most of the experiments. P. Jiang and S. Nakano established the *STX17* KO HeLa cells, and S. Nakano also performed the flow cytometry experiment. Y. Sakamaki carried out the electron microscopy experiment. T. Matsui and N. Mizushima wrote the manuscript. All authors analyzed and discussed the results and commented on the manuscript.

Submitted: 12 December 2017
Revised: 1 April 2018
Accepted: 7 May 2018

References

Abada, A., and Z. Elazar. 2014. Getting ready for building: signaling and autophagosome biogenesis. *EMBO Rep.* 15:839–852. https://doi.org/10.15252/embr.201439076

Barysch, S.V., R. Jahn, and S.O. Rizzoli. 2010. A fluorescence-based in vitro assay for investigating early endosome dynamics. *Nat. Protoc.* 5:1127–1137. https://doi.org/10.1038/nprot.2010.84

Blommaart, E.F., U. Krause, J.P. Schellens, H. Vreeling-Sindelárová, and A.J. Meijer. 1997. The phosphatidylinositol 3-kinase inhibitors wortmannin and LY294002 inhibit autophagy in isolated rat hepatocytes. *Eur. J. Biochem.* 243:240–246. https://doi.org/10.1111/j.1432-1033.1997.0240a.x

Cheng, X.T., B. Zhou, M.Y. Lin, Q. Cai, and Z.H. Sheng. 2015. Axonal autophagosomes recruit dynein for retrograde transport through fusion with late endosomes. *J. Cell Biol.* 209:377–386. https://doi.org/10.1083/jcb.201412046

De Leo, M.G., L. Staiano, M. Vicinanza, A. Luciani, A. Carissimo, M. Mutarelli, A. Di Campli, E. Polishchuk, G. Di Tullio, V. Morra, et al. 2016. Autophagosome-lysosome fusion triggers a lysosomal response mediated by TLR9 and controlled by OCRL. *Nat. Cell Biol.* 18:839–850. https://doi.org/10.1038/ncb3386

Diao, J., R. Liu, Y. Rong, M. Zhao, J. Zhang, Y. Lai, Q. Zhou, L.M. Wilz, J. Li, S. Vivona, et al. 2015. ATG14 promotes membrane tethering and fusion of autophagosomes to endolysosomes. *Nature.* 520:563–566. https://doi.org/10.1038/nature14147

Dilcher, M., B. Köhler, and G.F. von Mollard. 2001. Genetic interactions with the yeast Q-SNARE VTI1 reveal novel functions for the R-SNARE YKT6. *J. Biol. Chem.* 276:34537–34544. https://doi.org/10.1074/jbc.M101551200

Fukasawa, M., O. Varlamov, W.S. Eng, T.H. Söllner, and J.E. Rothman. 2004. Localization and activity of the SNARE Ykt6 determined by its regulatory domain and palmitoylation. *Proc. Natl. Acad. Sci. USA.* 101:4815–4820. https://doi.org/10.1073/pnas.0401183101

Gan, B., X. Peng, T. Nagy, A. Alcaraz, H. Gu, and J.L. Guan. 2006. Role of FIP200 in cardiac and liver development and its regulation of TNFalpha and

TSC-mTOR signaling pathways. *J. Cell Biol.* 175:121–133. https://doi.org/10.1083/jcb.200604129

Guo, B., Q. Liang, L. Li, Z. Hu, F. Wu, P. Zhang, Y. Ma, B. Zhao, A.L. Kovács, Z. Zhang, et al. 2014. O-GlcNAc-modification of SNAP-29 regulates autophagosome maturation. *Nat. Cell Biol.* 16:1215–1226. https://doi.org/10.1038/ncb3066

Hasegawa, H., S. Zinsser, Y. Rhee, E.O. Vik-Mo, S. Davanger, and J.C. Hay. 2003. Mammalian ykt6 is a neuronal SNARE targeted to a specialized compartment by its profilin-like amino terminal domain. *Mol. Biol. Cell.* 14:698–720. https://doi.org/10.1091/mbc.e02-09-0556

Hong, W. 2005. SNAREs and traffic. *Biochim. Biophys. Acta.* 1744:120–144. https://doi.org/10.1016/j.bbamcr.2005.03.014

Itakura, E., C. Kishi-Itakura, and N. Mizushima. 2012. The hairpin-type tail-anchored SNARE syntaxin 17 targets to autophagosomes for fusion with endosomes/lysosomes. *Cell.* 151:1256–1269. https://doi.org/10.1016/j.cell.2012.11.001

Jahn, R., and R.H. Scheller. 2006. SNAREs--engines for membrane fusion. *Nat. Rev. Mol. Cell Biol.* 7:631–643. https://doi.org/10.1038/nrm2002

Jiang, P., T. Nishimura, Y. Sakamaki, E. Itakura, T. Hatta, T. Natsume, and N. Mizushima. 2014. The HOPS complex mediates autophagosome-lysosome fusion through interaction with syntaxin 17. *Mol. Biol. Cell.* 25:1327–1337. https://doi.org/10.1091/mbc.e13-08-0447

Kabeya, Y., N. Mizushima, T. Ueno, A. Yamamoto, T. Kirisako, T. Noda, E. Kominami, Y. Ohsumi, and T. Yoshimori. 2000. LC3, a mammalian homologue of yeast Apg8p, is localized in autophagosome membranes after processing. *EMBO J.* 19:5720–5728. https://doi.org/10.1093/emboj/19.21.5720

Kaizuka, T., H. Morishita, Y. Hama, S. Tsukamoto, T. Matsui, Y. Toyota, A. Kodama, T. Ishihara, T. Mizushima, and N. Mizushima. 2016. An Autophagic Flux Probe that Releases an Internal Control. *Mol. Cell.* 64:835–849. https://doi.org/10.1016/j.molcel.2016.09.037

Kim, B.Y., H. Krämer, A. Yamamoto, E. Kominami, S. Kohsaka, and C. Akazawa. 2001. Molecular characterization of mammalian homologues of class C Vps proteins that interact with syntaxin-7. *J. Biol. Chem.* 276:29393–29402. https://doi.org/10.1074/jbc.M101778200

Kuma, A., M. Hatano, M. Matsui, A. Yamamoto, H. Nakaya, T. Yoshimori, Y. Ohsumi, T. Tokuhisa, and N. Mizushima. 2004. The role of autophagy during the early neonatal starvation period. *Nature.* 432:1032–1036. https://doi.org/10.1038/nature03029

Kweon, Y., A. Rothe, E. Conibear, and T.H. Stevens. 2003. Ykt6p is a multifunctional yeast R-SNARE that is required for multiple membrane transport pathways to the vacuole. *Mol. Biol. Cell.* 14:1868–1881. https://doi.org/10.1091/mbc.e02-10-0687

Lamb, C.A., T. Yoshimori, and S.A. Tooze. 2013. The autophagosome: origins unknown, biogenesis complex. *Nat. Rev. Mol. Cell Biol.* 14:759–774. https://doi.org/10.1038/nrm3696

Lee, S., Y. Sato, and R.A. Nixon. 2011. Lysosomal proteolysis inhibition selectively disrupts axonal transport of degradative organelles and causes an Alzheimer's-like axonal dystrophy. *J. Neurosci.* 31:7817–7830. https://doi.org/10.1523/JNEUROSCI.6412-10.2011

Mauvezin, C., P. Nagy, G. Juhász, and T.P. Neufeld. 2015. Autophagosome-lysosome fusion is independent of V-ATPase-mediated acidification. *Nat. Commun.* 6:7007. https://doi.org/10.1038/ncomms8007

Mauvezin, C., A.L. Neisch, C.I. Ayala, J. Kim, A. Beltrame, C.R. Braden, M.K. Gardner, T.S. Hays, and T.P. Neufeld. 2016. Coordination of autophagosome-lysosome fusion and transport by a Klp98A-Rab14 complex in Drosophila. *J. Cell Sci.* 129:971–982. https://doi.org/10.1242/jcs.175224

McEwan, D.G., D. Popovic, A. Gubas, S. Terawaki, H. Suzuki, D. Stadel, F.P. Coxon, D. Miranda de Stegmann, S. Bhogaraju, K. Maddi, et al. 2015. PLEKHM1 regulates autophagosome-lysosome fusion through HOPS complex and LC3/GABARAP proteins. *Mol. Cell.* 57:39–54. https://doi.org/10.1016/j.molcel.2014.11.006

McLelland, G.L., S.A. Lee, H.M. McBride, and E.A. Fon. 2016. Syntaxin-17 delivers PINK1/parkin-dependent mitochondrial vesicles to the endolysosomal system. *J. Cell Biol.* 214:275–291. https://doi.org/10.1083/jcb.201603105

McNew, J.A., M. Sogaard, N.M. Lampen, S. Machida, R.R. Ye, L. Lacomis, P. Tempst, J.E. Rothman, and T.H. Söllner. 1997. Ykt6p, a prenylated SNARE essential for endoplasmic reticulum-Golgi transport. *J. Biol. Chem.* 272:17776–17783. https://doi.org/10.1074/jbc.272.28.17776

Mizushima, N., and M. Komatsu. 2011. Autophagy: renovation of cells and tissues. *Cell.* 147:728–741. https://doi.org/10.1016/j.cell.2011.10.026

Mullock, B.M., C.W. Smith, G. Ihrke, N.A. Bright, M. Lindsay, E.J. Parkinson, D.A. Brooks, R.G. Parton, D.E. James, J.P. Luzio, and R.C. Piper. 2000. Syntaxin 7 is localized to late endosome compartments, associates with Vamp 8, and Is required for late endosome-lysosome fusion. *Mol. Biol. Cell.* 11:3137–3153 http://dx.doi.org/DOI 10.1091/mbc.11.9.3137. https://doi.org/10.1091/mbc.11.9.3137

Nair, U., A. Jotwani, J. Geng, N. Gammoh, D. Richerson, W.L. Yen, J. Griffith, S. Nag, K. Wang, T. Moss, et al. 2011. SNARE proteins are required for macroautophagy. *Cell.* 146:290–302. https://doi.org/10.1016/j.cell.2011.06.022

Nguyen, T.N., B.S. Padman, J. Usher, V. Oorschot, G. Ramm, and M. Lazarou. 2016. Atg8 family LC3/GABARAP proteins are crucial for autophagosome-lysosome fusion but not autophagosome formation during PINK1/Parkin mitophagy and starvation. *J. Cell Biol.* 215:857–874. https://doi.org/10.1083/jcb.201607039

Overly, C.C., and P.J. Hollenbeck. 1996. Dynamic organization of endocytic pathways in axons of cultured sympathetic neurons. *J. Neurosci.* 16:6056–6064. https://doi.org/10.1523/JNEUROSCI.16-19-06056.1996

Pryor, P.R., B.M. Mullock, N.A. Bright, M.R. Lindsay, S.R. Gray, S.C. Richardson, A. Stewart, D.E. James, R.C. Piper, and J.P. Luzio. 2004. Combinatorial SNARE complexes with VAMP7 or VAMP8 define different late endocytic fusion events. *EMBO Rep.* 5:590–595. https://doi.org/10.1038/sj.embor.7400150

Pryor, P.R., L. Jackson, S.R. Gray, M.A. Edeling, A. Thompson, C.M. Sanderson, P.R. Evans, D.J. Owen, and J.P. Luzio. 2008. Molecular basis for the sorting of the SNARE VAMP7 into endocytic clathrin-coated vesicles by the ArfGAP Hrb. *Cell.* 134:817–827. https://doi.org/10.1016/j.cell.2008.07.023

Rossi, V., D.K. Banfield, M. Vacca, L.E. Dietrich, C. Ungermann, M. D'Esposito, T. Galli, and F. Filippini. 2004. Longins and their longin domains: regulated SNAREs and multifunctional SNARE regulators. *Trends Biochem. Sci.* 29:682–688. https://doi.org/10.1016/j.tibs.2004.10.002

Ruiz-Martinez, M., A. Navarro, R.M. Marrades, N. Viñolas, S. Santasusagna, C. Muñoz, J. Ramírez, L. Molins, and M. Monzo. 2016. YKT6 expression, exosome release, and survival in non-small cell lung cancer. *Oncotarget.* 7:51515–51524. https://doi.org/10.18632/oncotarget.9862

Saitoh, T., H. Nakano, N. Yamamoto, and S. Yamaoka. 2002. Lymphotoxin-beta receptor mediates NEMO-independent NF-kappa B activation. *Febs Letters.* 532:45-51. http://dx.doi.org/Pii S0014-5793(02)03622-0.

Schindelin, J., I. Arganda-Carreras, E. Frise, V. Kaynig, M. Longair, T. Pietzsch, S. Preibisch, C. Rueden, S. Saalfeld, B. Schmid, et al. 2012. Fiji: an open-source platform for biological-image analysis. *Nat. Methods.* 9:676–682. https://doi.org/10.1038/nmeth.2019

Sou, Y.S., S. Waguri, J. Iwata, T. Ueno, T. Fujimura, T. Hara, N. Sawada, A. Yamada, N. Mizushima, Y. Uchiyama, et al. 2008. The Atg8 conjugation system is indispensable for proper development of autophagic isolation membranes in mice. *Mol. Biol. Cell.* 19:4762–4775. https://doi.org/10.1091/mbc.e08-03-0309

Tai, G., L. Lu, T.L. Wang, B.L. Tang, B. Goud, L. Johannes, and W. Hong. 2004. Participation of the syntaxin 5/Ykt6/GS28/GS15 SNARE complex in transport from the early/recycling endosome to the trans-Golgi network. *Mol. Biol. Cell.* 15:4011–4022. https://doi.org/10.1091/mbc.e03-12-0876

Takáts, S., P. Nagy, Á. Varga, K. Pircs, M. Kárpáti, K. Varga, A.L. Kovács, K. Hegedűs, and G. Juhász. 2013. Autophagosomal Syntaxin17-dependent lysosomal degradation maintains neuronal function in Drosophila. *J. Cell Biol.* 201:531–539. https://doi.org/10.1083/jcb.201211160

Takáts, S., K. Pircs, P. Nagy, Á. Varga, M. Kárpáti, K. Hegedűs, H. Kramer, A.L. Kovács, M. Sass, and G. Juhász. 2014. Interaction of the HOPS complex with Syntaxin 17 mediates autophagosome clearance in Drosophila. *Mol. Biol. Cell.* 25:1338–1354. https://doi.org/10.1091/mbc.e13-08-0449

Tochio, H., M.M. Tsui, D.K. Banfield, and M. Zhang. 2001. An autoinhibitory mechanism for nonsyntaxin SNARE proteins revealed by the structure of Ykt6p. *Science.* 293:698–702. https://doi.org/10.1126/science.1062950

Tsuboyama, K., I. Koyama-Honda, Y. Sakamaki, M. Koike, H. Morishita, and N. Mizushima. 2016. The ATG conjugation systems are important for degradation of the inner autophagosomal membrane. *Science.* 354:1036–1041. https://doi.org/10.1126/science.aaf6136

Uematsu, M., T. Nishimura, Y. Sakamaki, H. Yamamoto, and N. Mizushima. 2017. Accumulation of undegraded autophagosomes by expression of dominant-negative STX17 (syntaxin 17) mutants. *Autophagy.* 13:1452–1464. https://doi.org/10.1080/15548627.2017.1327940

Ungermann, C., G.F. von Mollard, O.N. Jensen, N. Margolis, T.H. Stevens, and W. Wickner. 1999. Three v-SNAREs and two t-SNAREs, present in a pentameric cis-SNARE complex on isolated vacuoles, are essential for homotypic fusion. *J. Cell Biol.* 145:1435–1442. https://doi.org/10.1083/jcb.145.7.1435

Volchuk, A., M. Ravazzola, A. Perrelet, W.S. Eng, M. Di Liberto, O. Varlamov, M. Fukasawa, T. Engel, T.H. Söllner, J.E. Rothman, and L. Orci. 2004.

Countercurrent distribution of two distinct SNARE complexes mediating transport within the Golgi stack. *Mol. Biol. Cell.* 15:1506–1518. https://doi.org/10.1091/mbc.e03-08-0625

Wang, Z., G. Miao, X. Xue, X. Guo, C. Yuan, Z. Wang, G. Zhang, Y. Chen, D. Feng, J. Hu, and H. Zhang. 2016. The Vici Syndrome Protein EPG5 Is a Rab7 Effector that Determines the Fusion Specificity of Autophagosomes with Late Endosomes/Lysosomes. *Mol. Cell.* 63:781–795. https://doi.org/10.1016/j.molcel.2016.08.021

Zhang, T., and W. Hong. 2001. Ykt6 forms a SNARE complex with syntaxin 5, GS28, and Bet1 and participates in a late stage in endoplasmic reticulum-Golgi transport. *J. Biol. Chem.* 276:27480–27487. https://doi.org/10.1074/jbc.M102786200